Available online at www.sciencedirect.com

ScienceDirect

journal homepage: www.jfda-online.com

Original Article

Characterization of titanium dioxide and zinc oxide nanoparticles in sunscreen powder by comparing different measurement methods

P.J. Lu [a], *S.W. Fang* [a,*], *W.L. Cheng* [a], *S.C. Huang* [a], *M.C. Huang* [b], *H.F. Cheng* [a]

[a] *Food and Drug Administration, Ministry of Health and Welfare, Taipei, Taiwan*
[b] *PerkinElmer Taiwan Corporation, Taipei, Taiwan*

ARTICLE INFO

Article history:
Received 25 August 2017
Received in revised form
18 January 2018
Accepted 23 January 2018
Available online 15 February 2018

Keywords:
Sunscreen powder
Nanoparticles
Titanium dioxide
Zinc oxide
Single particle inductively coupled plasma

ABSTRACT

Numerous consumer products, such as cosmetics, contain nanoparticles (NPs) of titanium dioxide (TiO_2) or zinc oxide (ZnO); however, this raises questions concerning the safety of such additives. Most of these products do not indicate whether the product includes NPs. In this study, we characterized metal oxide NPs according to size, shape, and composition as well as their aggregation/agglomeration characteristics. In order to comprehend quickly the characterization of metal oxide NPs, we employed single particle inductively coupled plasma (SP-ICPMS) to help quantify the size of metal oxide NPs; then, we use transmission electron microscopy (TEM) to corroborate the results. The crystal size and structure was measured by X-ray diffraction (XRD), there are two crystal phase of TiO_2 NPs in sunscreen powder showed in XRD. However, SP-ICPMS proved highly effective in determining the size of NPs, the results of which remarkably good agreement with the TEM measurements. Pre-treatment included a conventional copper grid (requiring sample dilution) to evaluate the size, shape and composition of primary particles or plastic embedding (without the need for sample dilution) to evaluate the aggregate/aggregation of native NOAAs. The proposed method is an effective and fast approach to the characterization of oxide NPs in cosmetic sunscreen powder. These findings outline an alternative approach to the analysis of NPs in powder-form matrix.

* Corresponding author. Food and Drug Administration, Ministry of Health and Welfare, No.161-2, Kunyang St, Nangang District, Taipei City 115-61, Taiwan, ROC. Fax: +886 2 2653 1764.
E-mail address: swf0204@fda.gov.tw (S.W. Fang).

https://doi.org/10.1016/j.jfda.2018.01.010

1. Introduction

Nanotechnology is widely used in cosmetic products, such as sunscreen and sunscreen powder. A lack of product labeling pertaining to nano-particles (NPs) means that consumers have no idea whether they are being exposed to nanomaterials. A large number of cosmetics that include NPs are high value-added items; however, they enjoy a time to market shorter than that of pharmaceuticals, which must undergo clinical evaluations [1].

According to the International Cooperation on Cosmetic Regulations (ICCR) [2], TiO_2 and ZnO NPs are used as inorganic UV filters in numerous personal care products. Metal oxide NPs are commonly used in sunscreen to provide broad-spectrum UV blocking without sacrificing transparency. NPs are a viable alternative to chemical UV filters, which pose the possibility of adverse health effects [3,4]. Furthermore, products that use NPs provide better texture, spread ability, and UV protection [5]. Nonetheless, NPs may also pose a threat to human health as well as the environment.

Under regulation (EC) No 1223/2009, the European parliament mandated the labeling of cosmetics that include NPs, starting on 11 July 2013 [6]. Commercial products containing nanomaterials must be registered at least six months prior to being released on the market. This labeling must include the name of the chemicals involved (IUPAC) as well as the size, physicochemical information, and toxicity. This has underlined the need for analytical methods with which to detect and characterize the nanomaterials used in cosmetics. The technical report from International Organization for Standardization (ISO) underlined the importance of physicochemical characterization in identifying such materials prior to toxicological testing. Particle size/particle size distribution, aggregation/agglomeration state, shape, surface area, composition, surface chemistry, surface charge, and solubility/dispersibility were listed as the physicochemical parameters [7]. The US FDA also emphasized the physicochemical properties and aggregation/agglomeration of nanoparticles in final cosmetic products [8]. It would be preferable to assess NPs in an unmodified state in order to prevent analytical artefacts associated with changes in the viscosity, aggregation/agglomeration, or the pH of the final products. The complexity and opacity of sunscreen formulations may also encumber efforts at characterization.

We previously investigated TiO_2 and ZnO NPs in liquid form (sprays, lotions, and creams) using XRD and TEM techniques [9–11]. To both observe sizing characterization and counting inorganic NPs more efficiently, single particle inductively coupled plasma-mass spectrometry (SP-ICPMS) is widely use in nano technology these few years. Thus, the aim of this study was investigated the feasibility of using XRD, SP-ICPMS, and TEM to analyze NPs in products in powdered form. No previous study has sought to characterize TiO_2 and ZnO NPs in sunscreen powder. First at all, the crystal phase was showed in XRD result. Then, we used SP-ICPMS which can quick and efficient know the mean size and size distribution of TiO_2 and ZnO NPs in sunscreen powder. In addition, the characterization of particle size, particle size distribution, shape, and aggregation/agglomeration were analysed by TEM to make sure the data of SP-ICPMS. Our results provide a valuable reference to guide the further application of NPs in a variety of cosmetic products.

2. Materials and methods

2.1. Sunscreen powder samples and standard nanoparticle controls

This study examined nine commercial sunscreen powders containing TiO_2 and/or ZnO, none of which provide any size-related information on the labels. Four of the samples contained only TiO_2 NPs and five contained a combination of TiO_2 and ZnO NPs, as shown in Table 1 All of these sunscreen products are available without prescription in Taiwan. Two products were made in the USA, seven products were made in Japan, and one product was made in Taiwan. We also purchased from Alfa Aesar (USA) standard TiO_2 powder that includes anatase and rutile crystals for the analysis of crystal structure. Standard solutions of ZnO NPs (76 nm) purchased from Sigma–Aldrich (USA) were also used for the analysis of crystal structure. We used NIST standard reference material (SRM) 1898 (mixed-phase nanocrystalline TiO_2) in powder form as a size control to verify the measurement methods. This SRM consisted of anatase and rutile crystals with an average size of 19 ± 2 nm and 37 ± 6 nm, as measured using XRD. The characteristic reflection patterns were 200 for anatase and 111 for rutile.

2.2. X-ray diffraction

XRD patterns were obtained from the samples at room temperature using a PaNalytical Pro X'pert Pro XRD (Netherlands), equipped with Cu Kα radiation (λ = 1.54051 Å). Prior to the measurement, we used NIST standard reference material 1976b consisting of a sintered alumina disc for XRD calibration with respect to instrumental broadening against all 2θ angles to eliminate variability in intensity measurements. Unmodified sunscreen samples and NIST SRM 1898 were placed in a metal holder and flattened gently using a glass coverslip. All samples were processed under the same operating

Table 1 – Summary of commercial sunscreen powder samples tested in this investigation.

Product No.	Origin	Ingredients		SPF
		TiO_2	ZnO	
1	USA	15.35%	–[b]	35
2	Japan	13.84%	4.43%	26
3	Japan	?[a]	3.35%	35
4	Taiwan	13.52%	5%	23
5	Japan	13.99%	–[b]	20
6	Japan	?[a]	4%	16
7	Japan	13.01%	4.99%	21
8	Japan	12.47%	–[b]	20
9	USA	9.5	–[b]	20

[a] Indicates inclusion of ingredient.
[b] Indicates that the substance is not present.

parameters: step size: 0.03°; scanning speed; 0.07 steps/s; scan 2θ range; 20°–90°. Crystal size was calculated using the X-ray line broadening method. Data were matched for the determination of crystal-phase and smoothed for the background using X′ Pert High Score Plot software. The full width at half maximum (FWHM) of reflections was calculated using Origin 8 (OriginLap, USA). The reflection used for crystallize analysis were 010 (at 31.7° 2θ) for ZnO, 011 (at 25.2° 2θ) for anatase TiO_2, and 110 (at 27.4° 2θ) for rutile phase.

2.3. *Conventional transmission electron microscopy*

Prior to assessment, the magnification and scale markers of TEM instruments (JEOL JEM-2100F, Japan) were calibrated to ensure smooth instrument operation and validate all measurement procedures. A portion of the sunscreen sample was loaded into a centrifuge tube. N-hexane, isopropanol, acetone, and methanol were respectively added for the removal of the non-volatile organic matrix from the formulation. The washed precipitate was diluted using ethanol, in accordance with NIST SRM 1898. 10 μL drops of the resulting dispersions were loaded directly onto a 200-mesh carbon-coated copper grid and then wicked dry using filter paper before undergoing air-drying at room temperature overnight. The size and shape of the particles were analyzed at an acceleration voltage of 200 kV and imaged at 15,000–200,000× magnification. Element composition was determined using energy dispersive spectroscopy (EDS; EDAX phoenix, U.S.A.). Multiple images were collected to measure a minimum of 200 NPs from each sample. ImageJ software [12] was used to define the dimensions of the NPs. The average size, size distribution, and aspect ratio were calculated using Microsoft Excel software.

2.4. *Transmission electron microscopy with plastic embedding*

Lu et al. [9] utilized a window-type microchip K-kit for the observation of NOAAs (nano-objects and their aggregates/agglomerates) under wet conditions; i.e., unmodified liquid sunscreen. Unfortunately, a K-kit proved unsuitable for the observation of NOAAs in powder samples. We employed plastic embedding to enable the observation of NPs in their native state. Plastic embedding is generally employed in diagnostic pathology and biological research. The plastic embedding process proceeds through the following steps: fixation, post-fixation, dehydration, block staining, embedding, and the preparation of semi-thin and thin sections. We modified this process to facilitate the detection of native NOAAs in cosmetic products. Briefly, we embedded 200 mg of untreated samples using the Spurr's Kit with low viscosity embedding media purchased from Electron Microscopy Sciences. The suspension was mixed thoroughly under rotation for 8 h before undergoing centrifugation at 6000 rpm for 8 min. The mixture was processed twice using fresh Spurr's plastic, before being polymerized at 68 °C for 15 h. The resulting polymer block was trimmed to form a trapezoid before being sliced to a thickness of approximately 100 nm using ultramicrotome (Leica EM UC7) while immersed in water. A copper grid held by forceps was used to retrieve the sections from the water bath after being sliced and fix them in place. After air drying overnight, the NOAAs in the slices were imaged using TEM in order to obtain a statistical population of NPs in the unmodified samples.

2.5. *Sample preparation for SP-ICPMS analysis*

Due to the inorganic NPs obtained sunscreen powder which showed in the TEM images were usually being not homogeneous aggregates. Therefore, to get the homogeneous suspension by NPs in sunscreen powder, first at all approach 0.04 g or more of the sunscreen power sample was dispersed in 1% Triton X-100 aqueous solution. Then, the mixture solution was vortexed and sonicated 30 min to homogenize the suspension sample. Finally, the mixture solution was diluted with DI-water appropriately before the SP-ICPMS analysis [11,13]. The transport efficiency was measured by 60 nm AuNP standard solution which the particle concentration were diluted to 10^5 particles/mL. In addition, the calibration standards were established by 2, 5, 10 ppb Ti and Zn ions, respectively.

3. Results and discussion

3.1. *X-ray diffraction analysis*

XRD is a powerful, non-destructive technique used in the analysis of crystalline materials. The intensity and shape of the peaks in the XRD patterns are affected by grain size. XRD is insensitive to grain size greater exceeding 100 nm; however, a broadening in the line is observed in the diffraction patterns of particles of less than 100 nm [14] The mean crystallite size of NPs in the sunscreen powder was calculated using the X-ray line broadening method based on the Scherrer formula [15], under the assumption that the NPs do not present strain broadening. Size estimation was based on line-broadening with corrections for instrumental broadening in X-ray diffraction line. The mean crystallite size of NPs in the sunscreen powder was calculated using the X-ray line broadening method based on the Scherrer formula [15], under the assumption that the NPs do not present strain broadening. Size estimation was based on line-broadening with corrections for instrumental broadening in X-ray diffraction lines.

Fig. 1 presents the XRD diffraction patterns of ten samples and SRM 1898. The sizes of the NIST SRM 1898 diffractions [(101) and (200) for anatase, (110) and (111) for rutile] were 22.27 ± 0.12, 21.10 ± 0.22, 35.16 ± 0.54, and 40.67 ± 3.83, respectively ($n = 5$). The sizes of the characteristic reflections (200 for anatase and 111 for rutile) were in agreement with the standards in the NIST 1898 report, thereby providing confirmation of the XRD results, as shown in Table 2. To measure the size of the TiO_2 particles in the samples, we selected the strongest diffraction peaks of anatase phase at $2\theta = 25.2°$ (011 plane) and rutile phase (110 plane at $2\theta = 27.4°$). We selected the peak at 31.7° (010 plane) to analyze the size of the ZnO NPs. Among the samples, only the intensity of COM 7 was too weak to calculate the size according to the FWHM of peaks related to specific lattice plane dhkl. Most of the TiO_2 and ZnO NPs presented no signs of broadening, which corresponds to crystallite sizes exceeding 100 nm.

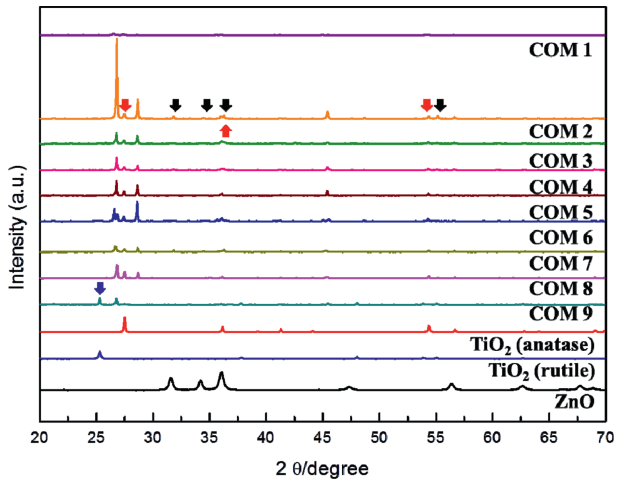

Fig. 1 – X-ray diffraction patterns of commercial sunscreen powder COM 1–9, illustrating anatase TiO_2, rutile TiO_2, and ZnO. Downward arrows indicate the 2θ positions for reflections from the rutile phase of TiO_2 and upward arrows indicate 2θ positions for reflections from ZnO wurtzite structures.

TiO_2 exists in three crystalline structures: anatase, rutile, and brookite. Rutile is the most common and stable form, with higher UV absorption and lower photoreactivity and toxicity than anatase [16–19]. XRD patterns reveal the existence of TiO_2 in all samples (rutile TiO_2 in COM 1-COM 8 and anatase TiO_2 in COM 9). The Scientific Committee on Consumer Safety (SCCS) reported that 10 out of 15 of the TiO_2 NPs they collected were rutile phase [20]. The same phase was identified in most of the samples in this investigation, which is a clear indication that rutile phase TiO_2, is prevalent in sunscreen products. This demonstrated that the proposed technique can be used to measure the size of particles in powder and liquid without the need for modification of the sunscreen beforehand. The proposed technique is also simple and cost effective.

3.2. *Conventional transmission electron microscopy*

Transmission electron microscopy (TEM) is listed in reports by the SCCS [21] and Organisation for Economic Co-operation and Development [22] as the preferred method for the characterization of nanomaterials. The SCCS recommended that at least two methods be applied for verification. TEM has been combined with EDS to measure the size, shape, and composition of particles in sunscreen powder products; however, this is only after the samples have undergone pre-treatment. TEM images present a clear edge around particles due to the fact that it is unaffected by the other ingredients in the samples (see Fig. 2). Nine out of ten samples in this study included TiO_2 particles of micro- (>100 nm) and nano-scale (<100 nm), whereas COM 5 included particles of 35.1 ± 10.7 nm. The size ZnO NPs in COM 3, COM 4, and COM 6 were 33.5 ± 20.7 nm, 86.9 ± 32.1 nm and 11.4 ± 5.5 nm, respectively. These values fit the standard definition of nanomaterials [6,23]. The International Cooperation on Cosmetic Regulations (ICCR) regards as

Table 2 – Results of XRD, TEM and SP-ICPMS analysis: Samples of commercial sunscreen powder.

Product No.	Particle	XRD		TEM				SP-ICPMS	
		Phase	PPS[a] (nm)	Particle size (nm)	Aspect ratio	Particle shape	Elements Detected by EDS	Most Freq. Size (nm)	Mean Size (nm)
COM 1	TiO_2	Rutile	>100	45.7 ± 14.0	5.36 ± 2.02	Needle shaped	Ti, C, O, Al, Si, (Cu)	45	53.29
				>100	–	Varied			
COM 2	TiO_2	Rutile	>100	33.7 ± 11.4	1.29 ± 0.26	Round shaped	Ti, Zn, Al, Si, (Cu)	25	38.17
				>100	–	Varied			
	ZnO	Wurtzite	>100	>100	–	Varied		40	46.54
COM 3	TiO_2	Rutile	>100	39.5 ± 14.0	4.74 ± 1.54	Needle shaped	Ti, Zn,C, O, Si, (Cu)	34	46.57
				>100	–	Varied			
	ZnO	Wurtzite	26	33.5 ± 20.7	1.30 ± 0.21	Varied		37	36.71
COM 4	TiO_2	Rutile	>100	49.6 ± 17.0	5.36 ± 1.92	Needle shaped	Ti, Zn,C, O, Si, (Cu)	30	39.48
				>100	–	Varied			
	ZnO	Wurtzite	77	86.9 ± 32.1	1.41 ± 0.35	Roundish		39	43.60
COM 5	TiO_2	Rutile	>100	35.1 ± 10.7	1.53 ± 0.36	Roundish	Ti, C, O, Si, (Cu)	29	45.68
				>100	–	Varied			
COM 6	TiO_2	Rutile	>100	42.5 ± 12.6	3.84 ± 1.34	Needle shaped	Ti, Zn,C, O, Mg,Al, Si, (Cu)	27	38.71
				>100	–	Varied			
	ZnO	–	–	11.4 ± 5.5	1.36 ± 0.26	Roundish		40	44.29
COM 7	TiO_2	Rutile	>100	30.9 ± 10.6	1.33 ± 0.23	Varied	Ti, Zn,C, O, Si, (Cu)	29	31.04
				>100	–	Varied			
	ZnO	Wurtzite	>100	>100	–	Varied		35	34.50
COM 8	TiO_2	Rutile	>100	>100	–	Varied	Ti, C, O, (Cu)	31	40.00
				>100	–	Rod			
COM 9	TiO_2	Anatase	>100	24.5 ± 8.1	1.59 ± 0.50	Roundish	Ti, C, O, Si, (Cu)	26	37.67
N-1898[b]	TiO_2	Anatase	22.27 ± 0.12	23.5 ± 10.0	1.15 ± 0.15	Roundish	Ti, C, O, (Cu)	–	
		Rutile	35.16 ± 0.54						

[a] PPS: Primary particle size.
[b] N-1898: NIST standard reference material 1898, the mean size vales obtained from the analysis of five randomly selected samples (n = 5).

Table 3 – Size distribution for TiO_2 NPs in commercial sunscreen powder measured at Day 1, Day 2 and Day 4.

Sample		Most Freq.		Mean Size		Part. Conc. (parts/mL)	
		Size (nm)	RSD (%)	Size (nm)	RSD (%)	(parts/mL)	RSD (%)
COM 1	Day 1	45	9.34	53.29	3.30	144,046	10.19
	Day 2	36		49.15		178,430	
	Day 4	43		51.10		182,062	
COM 2	Day 1	25	31.05	38.17	26.53	475,138	58.08
	Day 2	26		38.69		638,424	
	Day 4	47		65.04		85,209	
COM 3	Day 1	34	8.13	46.57	4.76	55,682	22.91
	Day 2	28		47.17		53,552	
	Day 4	30		42.32		86,235	
COM 4	Day 1	30	14.14	39.48	11.24	220,593	49.89
	Day 2	30		39.63		212,022	
	Day 4	40		49.81		47,196	
COM 5	Day 1	29	19.12	45.68	40.36	229,989	76.70
	Day 2	27		36.66		498,763	
	Day 4	41		89.61		26,984	
COM 6	Day 1	27	21.18	38.71	14.51	487,473	44.39
	Day 2	28		49.28		423,641	
	Day 4	42		55.52		132,661	
COM 7	Day 1	29	8.62	31.04	11.85	493,468	74.16
	Day 2	29		33.71		294,794	
	Day 4	24		40.92		11,594	
COM 8	Day 1	31	7.22	40.00	50.37	277,947	69.00
	Day 2	36		40.69		333,333	
	Day 4	31		107.29		7541	
COM 9	Day 1	26	18.21	37.67	49.86	453,494	65.70
	Day 2	23		38.52		512,950	
	Day 4	35		100.32		25,342	

Table 4 – Size distribution for ZnO NPs in commercial sunscreen powder measured at Day 1, Day 2 and Day 4.

Sample		Most Freq.		Mean Size		Part. Conc. (parts/mL)	
		Size (nm)	RSD (%)	Size (nm)	RSD (%)	(parts/mL)	RSD (%)
COM 2	Day 1	40	12.30	46.54	15.94	2363	89.38
	Day 2	38		40.69		7535	
	Day 4	50		59.33		308	
COM 3	Day 1	37	5.29	36.71	9.41	7148	53.29
	Day 2	33		33.05		8283	
	Day 4	37		41.57		1436	
COM 4	Day 1	39	12.60	43.60	17.47	865	133.55
	Day 2	37		36.81		27,668	
	Day 4	49		56.00		205	
COM 6	Day 1	40	4.51	44.29	8.42	807	73.92
	Day 2	37		36.40		6845	
	Day 4	36		38.43		2616	
COM 7	Day 1	35	3.43	34.50	3.34	16,197	34.59
	Day 2	36		36.53		7938	
	Day 4	38		37.38		8516	

nanomaterials any insoluble, intentionally manufactured ingredient with particles of which one or more dimensions range from 1 to 100 nm in the final formulation. Nine of the samples in this study contained both TiO_2 and ZnO particles with at least one dimension smaller than 100 nm.

Particle size alone is insufficient to articulate the state of the particles. The shape is also highly valuable in assessing the potential biological activity or quantifying the distribution characteristics [24]. The aspect ratio of particles expresses the relationship between length and width; i.e., the smallest aspect ratio would be 1:1 for perfectly round particles. We observed roundish and needle-shaped TiO_2 NPs as well as roundish and oddly shaped ZnO NPs in most of the samples (detailed in Table 2). Our findings were close to those in previous studies, which reported needle, spherical, or lanceolate TiO_2 particles and various isometric ZnO particles [3,20,25]. EDS analysis verified that TiO_2 and ZnO acted as mineral-based filters in all samples. We also observed Si or Al signals in most of the samples. Previous studies have reported the coating of mineral filters using silicon dioxide (SiO_2) or

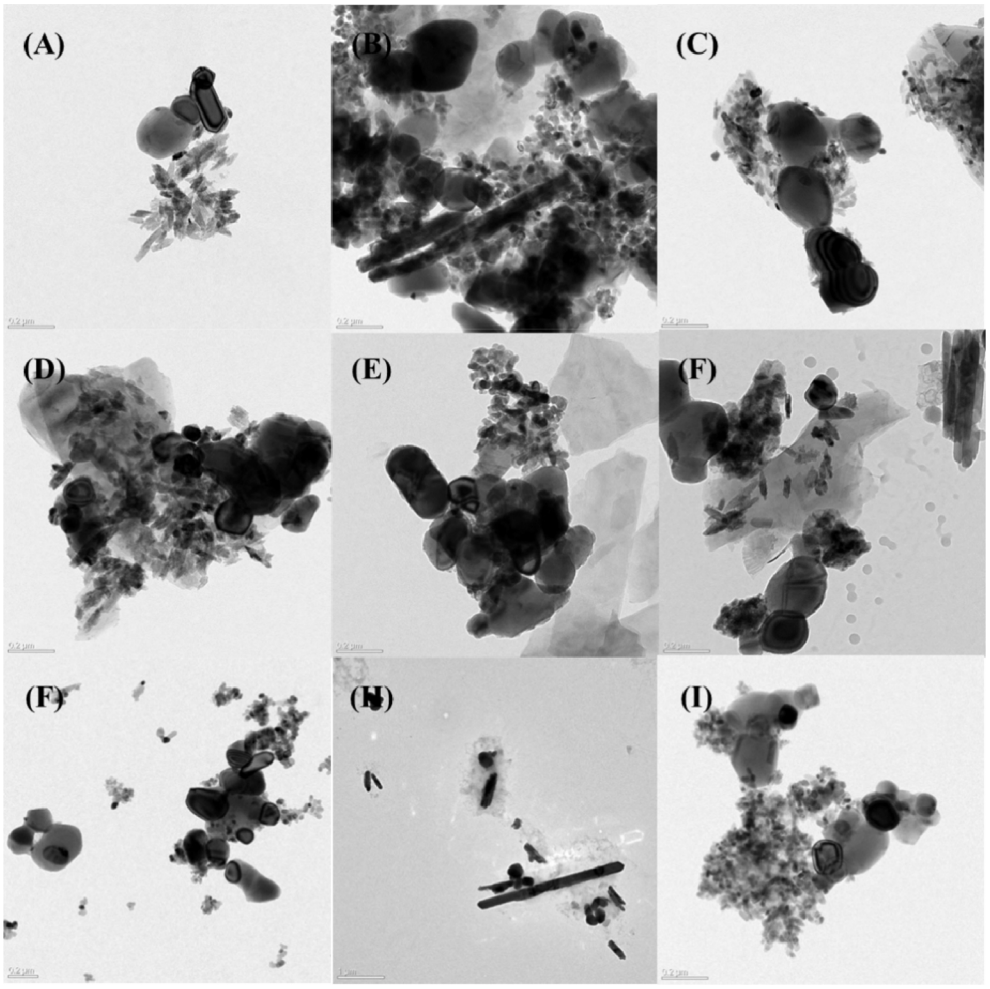

Fig. 2 – Images of commercial sunscreen powders containing inorganic NPs obtained using TEM with copper grids: (A) COM 1, (B) COM 2, (C) COM 3, (D) COM 4, (E) COM 5, (F) COM 6, (G) COM 7, (H) COM 8, and (I) COM 9. Images were acquired at a beam intensity of 200 kV and a magnification of 80,000 × –100,000 ×. The scale bar is 200 nm.

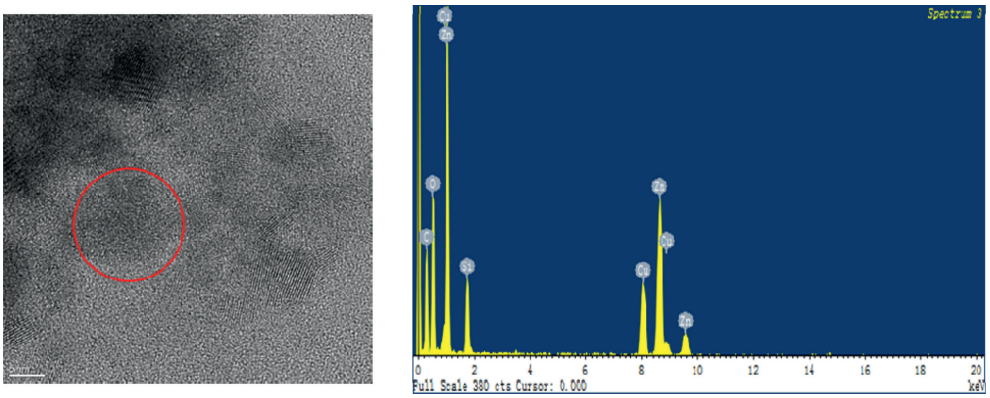

Fig. 3 – Images of commercial sunscreen powder COM 6 using transmission electron microscopy with copper grids. The circle indicates the area in which elemental analysis was performed. Images were acquired at a beam intensity of 200 kV and a magnification of 200,000 ×. The scale bar is 5 nm.

aluminum oxide (Al_2O_3) to reduce photoreactivity and minimize the formation of reactive oxygen species [3,26]. Another report listed the coating materials as follows: alumina/silica, methicone/silica, aluminium hydroxide and dimethicone/methicone copolymer, trimethyloctylsilane, alumina/silicone and alumina/silica/silicone, dimethicone, simethicone, dimethoxydiphenylsilane, triethoxycaprylylsilane. These coatings have been shown to improve the dispersion of TiO_2

NPs, inhibit or control photoactivity, and enhance compatibility with other ingredients [20]. Our results were in line with those reported in previous studies. Cu signal detected from the copper grids used in this study.

3.3. *Transmission electron microscopy with plastic embedding*

The FDA in the US recommends that any safety assessment of cosmetic products containing nanomaterials specify the aggregation/agglomeration of NPs in the final products [8]. TEM is a powerful tool for observing NPs; however, the fact that copper grids can artificially skew the distribution of particles means that this approach is seldom applied in the analysis of unmodified cosmetic products. Plastic embedding methods can also used in the preparation of cells and tissue to facilitate the observation of morphology using an electron microscopy, while minimizing the extraneous effects on the dispersion of particles [27]. Furthermore, the composition of NPs in a plastic-embedded specimen can be determined using an EDS detector.

Fig. 4 presents the NOAAs of TiO_2 and ZnO NPs in the unmodified sunscreen spray in COM 3. These results were obtained using TEM with the sample embedded within epoxy resin prior ultra-thin sectioning. We determined the aggregation/agglomeration state of native NOAAs of metal oxide NPs to provide a basis from which to conduct quantitative analysis on more than 150 particles. As shown in Table 5 and Fig. 4, the TiO_2 in COM 3 had an average particle size of 39.5 ± 14.0, whereas the ZnO NPs in COM 3 had an average particle size of 33.5 ± 20.7 nm. Agglomerations of TiO_2 NPs were observed in 100 of 182 studies (54.9%), presenting an average size of 115.7 ± 75.5 nm. Agglomerations of ZnO NPs were observed in 206 of 276 studies (74.6%) with an average size of 225.9 ± 100.2 nm. The ZnO NPs in COM 3 presented more obvious signs of agglomeration (Fig. 5). We compared the TEM data obtained using carbon-film-coated copper grids against the data obtained using plastic embedding. As shown in Table 5, the oxide NPs dried on copper grids were similar in size to those observed using the plastic embedding. Aggregates and agglomerates are regarded as secondary particles, whereas the original source particles are primary particles. Weakly-bonded agglomerates are more conducive to separation than are strongly-bonded aggregates. The size of aggregates/agglomerates in a sample has been shown to influence ADME behavior [7]. Our findings demonstrate that the use of plastic embedding in conjunction with TEM is a suitable approach to the characterization of aggregates/agglomerates of oxide NPs in sunscreen powder.

3.4. *Particle characterization in SP-ICPMS and comparison of size measurements*

SP-ICPMS is a rising technique, which can both sizing and counting inorganic NPs. Thus, it is widely use in nano technology such as, semiconductor, food, and costmotic [13,28,29]. Comparison of the size measurement between with XRD, TEM, and SP-ICPMS the result showed significant correlations (Table 2). The mean crystallite size of NPs in XRD indicated that some of NPs may occurred aggregate; thus, cause the primary particle size data in XRD almost exceeding 100 nm. On the other hand, TEM image also showed that the particle had strong aggregation in sunscreen powder caused the primary particle size of XRD was larger than 100 nm. In order to know the mean size of non-aggregates NPs which dimensions range from 1 to 100 nm. We selected at least 200 NPs alone and present a clear edge around particles unaffected by the other ingredients in the samples. The sizes indicated by XRD analysis was generally equal to or smaller than those obtained from TEM [27]. XRD measures the core of the coated NPs, rather than the surface coating, whereas TEM measures the overall size of the particles, including the surface coatings. The results in Table 2 illustrates that the XRD and TEM size values are in reasonable agreement in all of the samples except COM 6. TEM analysis indicated that the TiO_2 NPs in COM 6 were 11.4 ± 5.5 nm (Fig. 3), whereas XRD was unable to

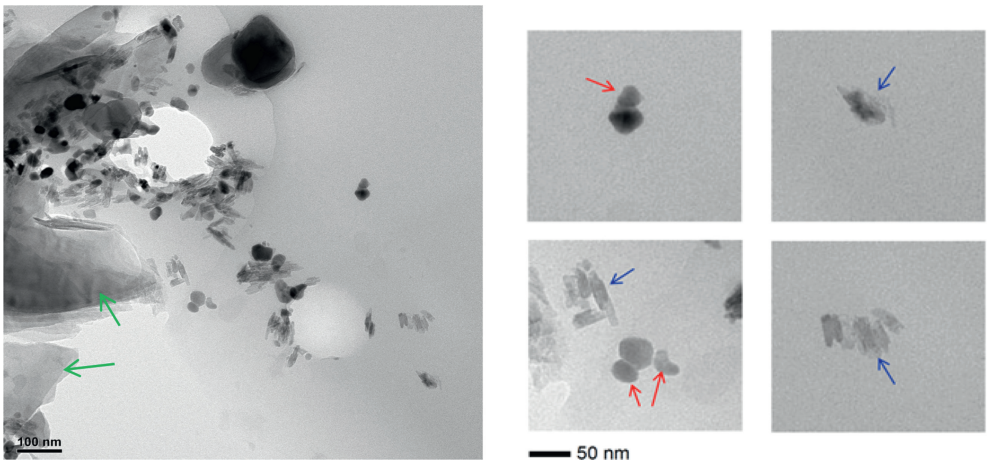

Fig. 4 – Characterization of NOAAs of TiO_2 and ZnO NPs in unmodified sunscreen powder COM 3, as determined using transmission electron microscopy with plastic embedding. Green arrows indicate non-target materials in the sample. The right image is an enlargement of the picture of the left. Blue arrows indicate the aggregation/agglomeration state of TiO_2 NPs and red arrows indicate the aggregation/agglomeration state of ZnO NPs. The scale bar is 50 nm.

Table 5 – Characterization of TiO_2 and ZnO NPs according to NOAAs in unmodified sunscreen powder COM 3 using TEM with plastic embedding/copper grid.

Particle Type		Size (nm)		Calculated number (%)	Calculated number	TEM images
		Average	Standard deviation			
Constituted particles						
Particle -1 (Ti/O)		39.5	14.0	100	226	Copper grid
Particle -2 (Zn/O)		33.5	20.7	100	234	
NOAAs[a] in products						
TiO_2	Nano-objects (NOs)	36.4	12.1	45	82	plastic embedding
	Aggregates/agglomerates (AAs)	115.7	75.5	55	100	
	NOAAs[a]	80.0	68.9	100	182	
ZnO	Nano-objects (NOs)	33.9	13.6	25	70	
	Aggregates/agglomerates (AAs)	225.9	100.2	75	206	
	NOAAs[a]	177.2	120.6	100	276	

[a] Nano-objects and their aggregates and agglomerates.

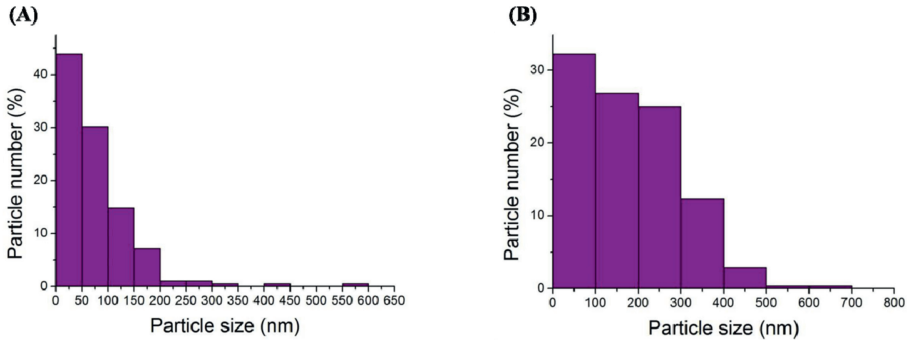

Fig. 5 – Size distribution of NPs, based on the average of the major and minor axes in unmodified sunscreen powder COM 3, as assessed by transmission electron microscopy with plastic embedding: (A) TiO_2 NPs; (B) ZnO NPs.

detect the particles at all. We speculate that the NPs were too small to produce a signal of sufficient intensity to stand out from the other components in the products, such as talc, mica and iron oxide. TEM analysis proved effective in revealing micro-as well as nanosized TiO_2 particles; however, XRD revealed only micro-sized particles. This can be attributed to the strong peaks shielding the weaker peaks, such that peak broadening was not apparent in the XRD patterns. According to ISO technical specifications, XRD can be used to measure the average crystal size of TiO_2, whereas TEM is used to measure the average primary particle size.

Although TEM measurement results also require the number of particles in order to obtain the average size and standard deviation, but it limit of quantitation just represented few number of particles. Consequently, we attempt used SP-ICPMS (PerkinElmer's NexION® 2000) to measure various sunscreen powder with different sun protection factor (SPF) and inorganic composition NPs. SP-ICPMS showed effective result that whether most frequency size or mean size symboled strong relationship with TEM (Table 2). To realize the stability of NPs, we measured the suspension for different days, COM 1, COM 3, COM 7, and COM 8 demonstrated good reproducibility in most frequency size. However, in the mean size only COM 1 and COM 3 illustrated reproducibility (Tables 3 and 4). Due to sunscreen products consist of many organic composition, which let the NPs easier become agglomeration cause the stability of NPs in sunscreen products cannot over two days. Nevertheless, extend the stability of NPs in sunscreen products still a necessarily challenge for SP-ICPMS analysis, but compared to XRD and TEM, SP-ICPMS show more accurately and efficiently; in addition, the huge amount of quantity make the data more convincing.

4. Conclusions

This study examined various approaches to assessing the physicochemical properties of TiO_2 and ZnO NPs (in powder form) in sunscreen powder. XRD was used to obtain the crystal structure and mean particle size in unmodified sunscreen powder. TEM was used in conjunction with copper grids or plastic embedding to measure the particle size, size distribution, shape, composition, and native aggregation/agglomeration status. They presented highly consistent sizing results and the two methods provide complementary information with respect to the characteristics of NPs in the sample, for example in sample COM 3 the primary particle size in XRD was over than 100 nm, whereas in TEM images showed that aggregations of the particles exceeded 100 nm which cause the result of XRD. Thus, XRD is unable to provide the accurate size analysis above 100 nm, should assisted by TEM to minimize aggregation/agglomeration of NPs, but it still existed some inherent limitations. To overcome the inherent limitations of TEM and XRD, SP-ICPMS analytical methods

which can highly effective in characterizing the NPs in sunscreen powder. In our study, SP-ICPMS result showed the most frequency size and mean size of the NPs in sunscreen powder, respectively. Both of the result demonstrated significant relationship between TEM and XRD. Compared to XRD despite both of them showed efficiently in analysis, but the accuracy of SP-ICPMS was more powerful. On the other hand, the quantity of NPs for test in SP-ICPMS was greater than TEM that make the size distribution of SP-ICPMS more convincing. In conclusion, SP-ICPMS was the best candidate in NPs analysis which showed the accurately and efficiently characteristic. Furthermore, TEM and XRD can not only support, but verify the data of SP-ICPMS. These findings outline an alternative approach to the analysis of NPs in matrix and powder-form.

Acknowledgements

[1] This work was supported by the grant MOHW104-FDA-N-114-000742 from Food and Drug Administration, Ministry of Health and Welfare in Taiwan, R.O.C.

[2] The authors would like to thank Mr. Y. Y. Chen of Institute of physics, academia sinica for his help with the XRD assessment.

REFERENCES

[1] Mihranyan A, Ferraz N, Strømme M. Current status and future prospects of nanotechnology in cosmetics. Prog Mater Sci 2012;57(5):875–910.
[2] ICCR. Report for international cooperation on cosmetic regulation: 2011 associations survey of nanomaterials used in cosmetic products. 2011.
[3] Lorenz C, Tiede K, Tear S, Boxall A, Von Goetz N, Hungerbühler K. Imaging and characterization of engineered nanoparticles in sunscreens by electron microscopy, under wet and dry conditions. Int J Occup Environ Health 2010;16(4):406–28.
[4] Morganti P. Use and potential of nanotechnology in cosmetic dermatology. Clin Cosmet Invest Dermatol CCID 2010;3:5–13.
[5] Singh P, Nanda A. Enhanced sun protection of nano-sized metal oxide particles over conventional metal oxide particles: an in vitro comparative study. Int J Cosmet Sci 2014;36(3):273–83.
[6] OJEU. Regulation (EC) No 1223/2009 of the European parliament and of the council of 30 November 2009 on cosmetic products. 2009.
[7] ISO. Nanotechnologies–Guidance on physico-chemical characterization of engineered nanoscale materials for toxicologic assessment. Int Org Stand 2012. ISO/TR 13014:2012.
[8] FDA. Guidance for industry: safety of nanomaterials in cosmetic products. 2014.
[9] Lu PJ, Cheng WL, Huang SC, Chen YP, Chou HK, Cheng HF. Characterizing titanium dioxide and zinc oxide nanoparticles in sunscreen spray. Int J Cosmet Sci 2015;37(6):620–6.
[10] Lu P-J, Huang S-C, Chen Y-P, Chiueh L-C, Yang-Chih SD. Analysis of titanium dioxide and zinc oxide nanoparticles in cosmetics. J Food Drug Anal 2015;23(3):587–94.
[11] Dan Y, Shi H, Stephan C, Liang X. Rapid analysis of titanium dioxide nanoparticles in sunscreens using single particle inductively coupled plasma–mass spectrometry. Microchem J 2015;122:119–26.
[12] Rasband W. ImageJ software. 1997-2016. Available from: https://imagej.nih.gov/ij/docs/index.html.
[13] López-Heras I, Madrid Y, Cámara C. Prospects and difficulties in TiO_2 nanoparticles analysis in cosmetic and food products using asymmetrical flow field-flow fractionation hyphenated to inductively coupled plasma mass spectrometry. Talanta 2014;124:71–8.
[14] Wokovich A, Tyner K, Doub W, Sadrieh N, Buhse LF. Particle size determination of sunscreens formulated with various forms of titanium dioxide. Drug Dev Ind Pharm 2009;35(10):1180–9.
[15] Klug HP, Alexander LE. X-ray diffraction procedures: for polycrystalline and amorphous materials. Wiley; 1974.
[16] Smijs TG, Pavel S. Titanium dioxide and zinc oxide nanoparticles in sunscreens: focus on their safety and effectiveness. Nanotechnol Sci Appl 2011;4:95–112.
[17] Tyner KM, Wokovich AM, Godar DE, Doub WH, Sadrieh N. The state of nano-sized titanium dioxide (TiO_2) may affect sunscreen performance. Int J Cosmet Sci 2011;33(3):234–44.
[18] Themaa FT, Manikandan E, Dhlamini MS, Maaza M. Green synthesis of ZnO nanoparticles via Agathosma betulina natural extract. Mater Lett 2015;161:124–7.
[19] Fang F, Kennedy J, Manikandan E, Futter J, Markwitz A. Morphology and characterization of TiO_2 nanoparticles synthesized by arc discharge. Chem Phys Lett 2012;521:86–90.
[20] SCCS. Opinion on titanium dioxide(nano form). 2013.
[21] SCCS. Guidance on the safety assessment of nanomaterials in cosmetics. 2012.
[22] OECD. Report of the OECD expert meeting on the physical chemical properties of manufactured nanomaterials and test guidelines. 2014.
[23] ICCR. Report of the ICCR joint ad hoc working group on nanotechnology in cosmetic products: criteria and methods of detection - ICCR-4. 2010.
[24] ICCR. Report of the ICCR working group: safety approaches to nanomaterials in cosmetics. 2013.
[25] SCCS. Opinion on zinc oxide(nano form). 2012.
[26] Lewicka ZA, Benedetto AF, Benoit DN, Yu WW, Fortner JD, Colvin VL. The structure, composition, and dimensions of TiO_2 and ZnO nanomaterials in commercial sunscreens. J Nanoparticle Res 2011;13(9):3607–17.
[27] Graham L, Orenstein JM. Processing tissue and cells for transmission electron microscopy in diagnostic pathology and research. Nat Protoc 2007;2(10):2439–50.
[28] Pace HE, Rogers NJ, Jarolimek C, Coleman VA, Higgins CP, Ranville JF. Determining transport efficiency for the purpose of counting and sizing nanoparticles via single particle inductively coupled plasma mass spectrometry. Anal Chem 2011;83(24):9361–9.
[29] Singh G, Stephan C, Westerhoff P, Carlander D, Duncan TV. Measurement methods to detect, characterize, and quantify engineered nanomaterials in foods. Compr Rev Food Sci Food Saf 2014;13(4):693–704.